

4-22-2022

## Challenges in Kinetic-Kinematic Driven Musculoskeletal Subject-Specific Infant Modeling

Yeram Lim

*Embry-Riddle Aeronautical University, ydlim.3@gmail.com*

Victor Huayamave

*Embry-Riddle Aeronautical University, huayamav@erau.edu*

Tamara Chambers

*Embry-Riddle Aeronautical University, chambet2@my.erau.edu*

Christine Walck

*Embry-Riddle Aeronautical University, daileyc1@erau.edu*

Safeer Siddicky

*Boise State University, safeersiddicky@boisestate.edu*

*See next page for additional authors*

Follow this and additional works at: <https://commons.erau.edu/publication>



Part of the [Mechanical Engineering Commons](#)

---

### Scholarly Commons Citation

Lim, Y., Huayamave, V., Chambers, T., Walck, C., Siddicky, S., & Mannen, E. (2022). Challenges in Kinetic-Kinematic Driven Musculoskeletal Subject-Specific Infant Modeling. *Mathematical and Computational Applications*, 27(36). <https://doi.org/10.3390/mca27030036>

This Article is brought to you for free and open access by Scholarly Commons. It has been accepted for inclusion in Publications by an authorized administrator of Scholarly Commons. For more information, please contact [commons@erau.edu](mailto:commons@erau.edu).



---

**Authors**

Yeram Lim, Victor Huayamave, Tamara Chambers, Christine Walck, Safeer Siddicky, and Erin Mannen

Article

# Challenges in Kinetic-Kinematic Driven Musculoskeletal Subject-Specific Infant Modeling

Yeram Lim <sup>1</sup>, Tamara Chambers <sup>1</sup> , Christine Walck <sup>1</sup>, Safer Siddicky <sup>2,3</sup> , Erin Mannen <sup>2</sup>  
and Victor Huayamave <sup>1,\*</sup> 

<sup>1</sup> Department of Mechanical Engineering, Embry-Riddle Aeronautical University, Daytona Beach, FL 32114, USA; ydlim.3@gmail.com (Y.L.); chambet2@my.erau.edu (T.C.); daileyc1@erau.edu (C.W.)

<sup>2</sup> Mechanical and Biomedical Engineering Department, Boise State University, Boise, ID 83725, USA; safersiddicky@boisestate.edu (S.S.); erinmannen@boisestate.edu (E.M.)

<sup>3</sup> Department of Kinesiology and Health Education, The University of Texas at Austin, Austin, TX 78712, USA

\* Correspondence: huayamav@erau.edu

**Abstract:** Musculoskeletal computational models provide a non-invasive approach to investigate human movement biomechanics. These models could be particularly useful for pediatric applications where in vivo and in vitro biomechanical parameters are difficult or impossible to examine using physical experiments alone. The objective was to develop a novel musculoskeletal subject-specific infant model to investigate hip joint biomechanics during cyclic leg movements. Experimental motion-capture marker data of a supine-lying 2-month-old infant were placed on a generic GAIT 2392 OpenSim model. After scaling the model using body segment anthropometric measurements and joint center locations, inverse kinematics and dynamics were used to estimate hip ranges of motion and moments. For the left hip, a maximum moment of 0.975 Nm and a minimum joint moment of 0.031 Nm were estimated at 34.6° and 65.5° of flexion, respectively. For the right hip, a maximum moment of 0.906 Nm and a minimum joint moment of 0.265 Nm were estimated at 23.4° and 66.5° of flexion, respectively. Results showed agreement with reported values from the literature. Further model refinements and validations are needed to develop and establish a normative infant dataset, which will be particularly important when investigating the movement of infants with pathologies such as developmental dysplasia of the hip. This research represents the first step in the longitudinal development of a model that will critically contribute to our understanding of infant growth and development during the first year of life.

**Keywords:** musculoskeletal model; infant movement; biomechanics; motion capture; OpenSim



**Citation:** Lim, Y.; Chambers, T.; Walck, C.; Siddicky, S.; Mannen, E.; Huayamave, V. Challenges in Kinetic-Kinematic Driven Musculoskeletal Subject-Specific Infant Modeling. *Math. Comput. Appl.* **2022**, *27*, 36. <https://doi.org/10.3390/mca27030036>

Academic Editors: Simona Perotto, Gianluigi Rozza and Antonia Laresse

Received: 21 January 2022

Accepted: 19 April 2022

Published: 22 April 2022

**Publisher's Note:** MDPI stays neutral with regard to jurisdictional claims in published maps and institutional affiliations.



**Copyright:** © 2022 by the authors. Licensee MDPI, Basel, Switzerland. This article is an open access article distributed under the terms and conditions of the Creative Commons Attribution (CC BY) license (<https://creativecommons.org/licenses/by/4.0/>).

## 1. Introduction

Human movements are complex event sequences that involve high coordination levels between musculoskeletal and neurological systems. Establishing the normative characteristics of specific human movements is particularly important when investigating individuals who have pathologies preventing natural movements. In the biomechanics field, aspects of human movements, such as segmental kinematics, kinetics, and muscle activity, are experimentally quantified and characterized by using established methodologies, such as marker-based motion capture (MOCAP), inertial measurement units, force plates, and electromyography. While these technologies are non-invasive, they require the presence of human subjects in the laboratory following specific instructions to obtain a useful dataset. For common human movements such as walking gait, once normative experimental data ranges are established for specific populations, biomechanists often turn to musculoskeletal computational models (MCM). MCM are convenient to non-invasively study the simulated dynamics of human movement, bypassing the investigation of in vivo and in vitro

biomechanical parameters that may be difficult or impossible to examine using physical experiments alone.

Over the past two decades, the complexity and quality of MCM advanced at a rapid rate. In the biomechanics literature, MCMs have been used for a wide range of applications, including sports performance [1,2], clinical outcomes [3–8], occupational ergonomics [9,10], and accident reconstruction [11]. While there has been a steady advance in adult human MCM [12–14], neonatal and infant populations have been widely under-investigated in modeling.

In early infancy, when babies experience rapid development, it is vital to understand the nature of infant movements in daily body positioning environments and the effect on healthy musculoskeletal development. Novel MCMs have studied these effects during fetal movement [15–17] and pathological conditions in infancy, such as developmental dysplasia of the hip (DDH) [18–20]. DDH is an abnormal condition in infants characterized by dislocation, misalignment, or instability of the hip [21,22]. Infants are at a greater risk of DDH if they were in a breech position during delivery, are female, are the first-born, or have a family history of DDH [23]. Challenges in establishing a normative dataset are due to difficulties in recruiting infant subjects and the dearth of biomechanical studies examining movement and coordination in early infancy. Developing realistic infant MCM is crucial, particularly due to the paucity of experimental infant data in the literature. Additionally, since infants experience rapid growth in their first year of life, it is equally important to develop subject-specific infant MCM to obtain a more robust understanding of their movements and the subsequent joint and musculoskeletal development. MCM achieve the closest approximation to physiologically accurate movements when they are developed as subject-specific models. However, developing subject-specific MCM is a complicated, multi-layered process, often involving segmental anthropometric measurements, 3D imaging such as MRI/CT, 3D kinematics using MOCAP, and electromyography.

Typically, subject-specific MCMs are developed by scaling the generic model using the subject's segment anthropometries [24]. The segment lengths can be calculated using surface anatomical landmarks [24] alone or in combination with joint center locations. Kainz et al. [25] found that incorporating joint centers in the scaling process significantly increased the accuracy of the thigh and shank segment estimates when compared to scaling with surface markers alone. The hip joint center (HJC) locations are difficult to estimate because HJC locations cannot be directly identified from surface marker locations. HJC locations can be estimated using functional estimation methods or regression equations. Knee and ankle joint centers can also be estimated using functional methods. Functional approaches are implemented during MOCAP for subjects who have a sufficient hip range of motion and can easily perform the instructed functional movements [24]. However, regression equations are implemented after MOCAP for subjects who have a limited hip range of motion [24] or cannot perform the required movements. Both approaches are accepted methods of calculating HJC locations when medical imaging is not available [26], which is the case for infant populations under the age of one year where MRI/CT is unavailable.

Previous studies have attempted to quantify an infant's joint kinematics and kinetics during spontaneous movement, but an infant MCM has yet to be created. The purpose of this work was to develop a novel lower extremity computational musculoskeletal model representative of an infant, using body segment anthropometric measurements and experimental MOCAP data of a single infant taken from previously collected infant biomechanics data [27,28]. This study will provide more insight into biomechanical loadings at the hip joint during a spontaneous kick and will provide a noninvasive technique for evaluating the mechanisms contributing to infant hip development.

## 2. Materials and Methods

### 2.1. Experimental Methods

De-identified experimental data for one healthy, full-term male infant (2.4 months) was obtained from a study approved by the Institutional Review Board of the University of

Arkansas for Medical Sciences [28]. The infant was weighed on an infant scale at 5.35 kg and was measured head to heel (lying supine) at 56 cm. Leg length measurements were made with a standard measuring tape, with the right and left leg measuring 23 cm and 22 cm, respectively. Marker-based MOCAP (100 Hz; Vicon, Oxford, UK) recorded movement through reflective markers placed bilaterally on the anterior and posterior of the head, anterior superior iliac spine (ASIS), posterior superior iliac spine (PSIS), greater trochanter, medial and lateral epicondyles of the knee, and the medial and lateral malleolus of the ankle. Additionally, three-marker rigid bodies were placed on the anterior and posterior of the pelvis and bilaterally on the lateral aspect of each thigh. Data were recorded over a 30 s period with the infant lying in the supine position and was allowed to move freely and naturally without any external stimulations as shown in Figure 1a.

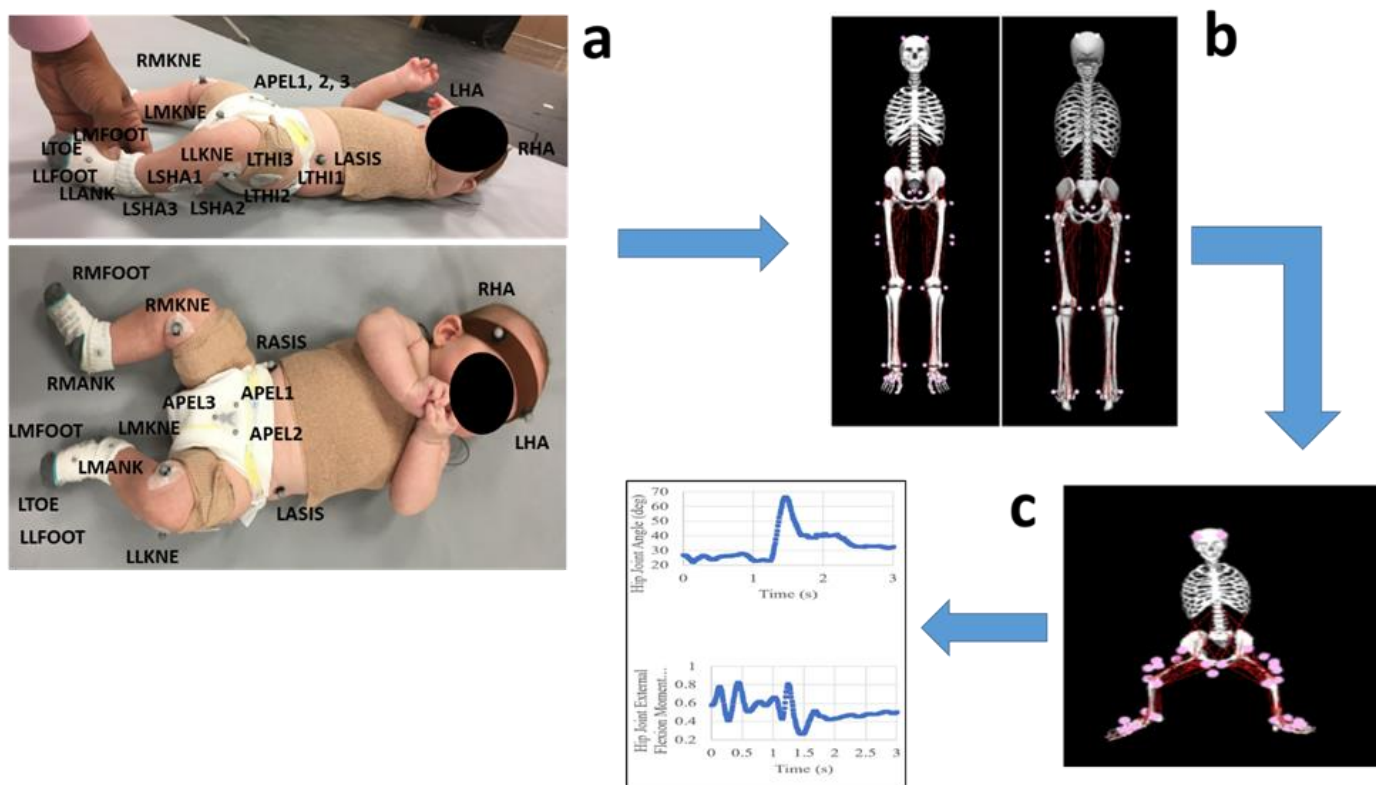


**Figure 1.** Methodology pipeline: (a) infant MOCAP data collection, (b) musculoskeletal scaling, and (c) musculoskeletal model to predict hip joint ROMs and external hip joint moments.

## 2.2. Musculoskeletal Model Development

Markers from the experiment were placed on a generic GAIT 2392 OpenSim model [29,30], which is used for simulating lower extremity dominant motions. This model has 23 degrees of freedom and 96 musculotendon actuators that represent 76 muscles in the lower extremity, including the pelvis, femur, tibia, fibula, talus, foot, and toes.

To create a subject-specific model representative of an infant's size, marker-based scaling was used. This scaling approach minimizes the distance between experimental and model (virtual) markers through optimization and predicts scale factors. The optimization used during scaling was a weighted least squares optimization problem given by Equation (1) [21], where  $q$  is the vector of generalized coordinates being solved for,  $x_i^{\text{exp}}$  is the experimental position of marker  $i$ ,  $x_i(q)$  is the position of the corresponding model marker (which depends on the coordinate values), and  $q_j^{\text{exp}}$  is the experimental value for coordinate  $j$ . The prescribed coordinates are set to their experimental values. The goal

of the optimization problem was to place the model markers in the position that closely matched the subject's position while minimizing marker errors.

$$\min_{\mathbf{q}} \left[ \sum_{i \in \text{markers}} w_i \|x_i^{\text{exp}} - x_i(\mathbf{q})\|^2 + \sum_{i \in \text{unprescribed coords}} w_j (q_j^{\text{exp}} - q_j)^2 \right] \quad (1)$$

$$q_j = q_j^{\text{exp}} \text{ for all prescribed coordinates } j$$

Functional joint centers for the hips, knees, and ankles were estimated and used during the scaling process. The ankle and knee joint centers were calculated using the midpoint between the medial and lateral marker positions. The hip joint centers (HJC) were estimated using regression equations based on the subject's leg length (LL) [31], as shown in Equations (2)–(4).

$$\text{HJC}_x = 11 - 0.063 \times \text{LL} \quad (2)$$

$$\text{HJC}_y = 8 + 0.086 \times \text{LL} \quad (3)$$

$$\text{HJC}_z = -9 - 0.078 \times \text{LL} \quad (4)$$

The mean absolute errors for the posterior-anterior ( $\text{HJC}_x$ ), medial-lateral ( $\text{HJC}_y$ ), and inferior-superior ( $\text{HJC}_z$ ) position equations are 5.2 mm, 4.4 mm, and 3.8 mm, respectively. The femur and tibia were both scaled non-uniformly by using a scale factor for the medial-lateral direction and the superior-inferior direction. Since the infant was placed in the supine position, the posterior pelvic markers were not captured during MOCAP. Thus, the pelvis was scaled uniformly with respect to the medial-lateral direction.

The average upper-segment lower-segment (USLS) infant ratio [32], which compares the upper segment (torso) and lower segment (legs), was also used to validate scaling. A 5% difference was found between the reported USLS infant ratio (1.70) and the scaled musculoskeletal model USLS infant ratio (1.61). In addition, a user-defined constant ground reaction force (GRF) was defined to represent the infant's weight normal to the ground and was applied at the infant's coccyx. The GRFs in the shear directions were neglected since the infant was lying supine and the motion was only observed in the lower extremity. Typically, generic models use a synchronous GRF during scaling obtained from a calibration sequence completed by the participant (either a static pose or a series of predefined functional movements). For infant MOCAP studies, infants are generally placed in a supine position, and there is not much variation in GRFs. Therefore, we assumed a constant GRF concentrated at the coccyx. Inverse kinematics and inverse dynamics were then used to estimate hip joint range of motion (ROM) and external moments. Figure 1 shows the methodology pipeline used in this study. Figure 2 shows the subject-specific musculoskeletal infant model.

### 2.3. Outcome Measures

A movement of the hip joint beginning from an extended position moving through a single flexion phase and then returning to the extended position is defined as a single kick. A single, discrete kick, defined by a kick where no other kicking motion is observed within 1 s before and after the kick, was identified and isolated over a 3 s period for each hip to visualize the extended–flexed–extended pattern [33]. To compare the kick on the left and right leg, the kick-start time was adjusted to plot the kicks generated by both the right and left hips.

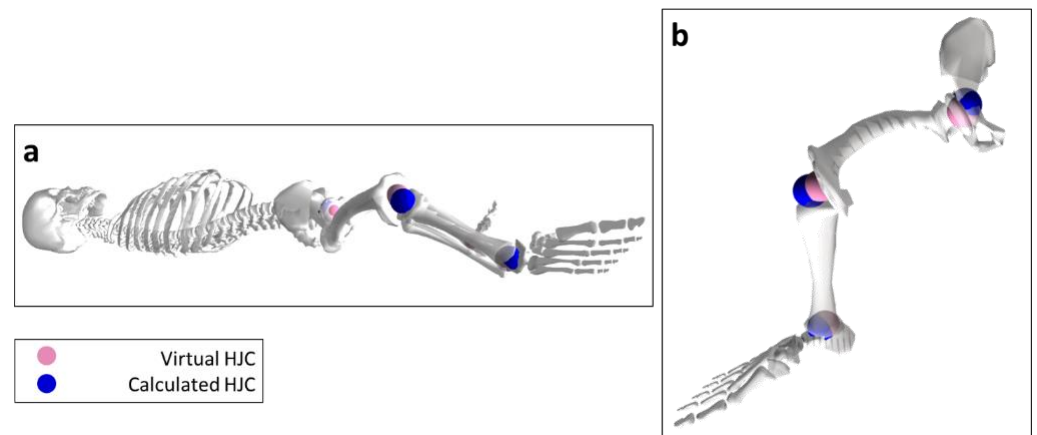


**Figure 2.** Subject-specific OpenSim model displaying the virtual joint center marker positions in pink and the calculated joint center marker positions in blue. (a) Right-side view of the musculoskeletal model in the supine position and (b) isolated right lower extremity. Head and torso bodies are not to scale.

### 3. Results

#### 3.1. Hip Joint Range of Motion

Over a 3 s period, minimum joint angle values of 22.2° (right hip) and 23.2° (left hip) and maximum joint angle values of 66.6° (right hip) and 66.3° (left hip) were predicted as shown in Figure 3. For both kicks, the maximum hip flexion was calculated to be approximately 66.0°. Additionally, Figure 4 shows the beginning and end of the kick cycle for both the right and left hips and identifies all different stages of the motion defined by each single kick, which was classified as discrete.

Once both kicks were classified, the cyclic data for the right hip and left hip were isolated again to show the beginning and end of the kick cycle. Figure 4 shows details of flexion and extension for both hips where the kick starts with the hip moving towards the trunk as it reaches maximum flexion and then moves away from the body as the hip extends.

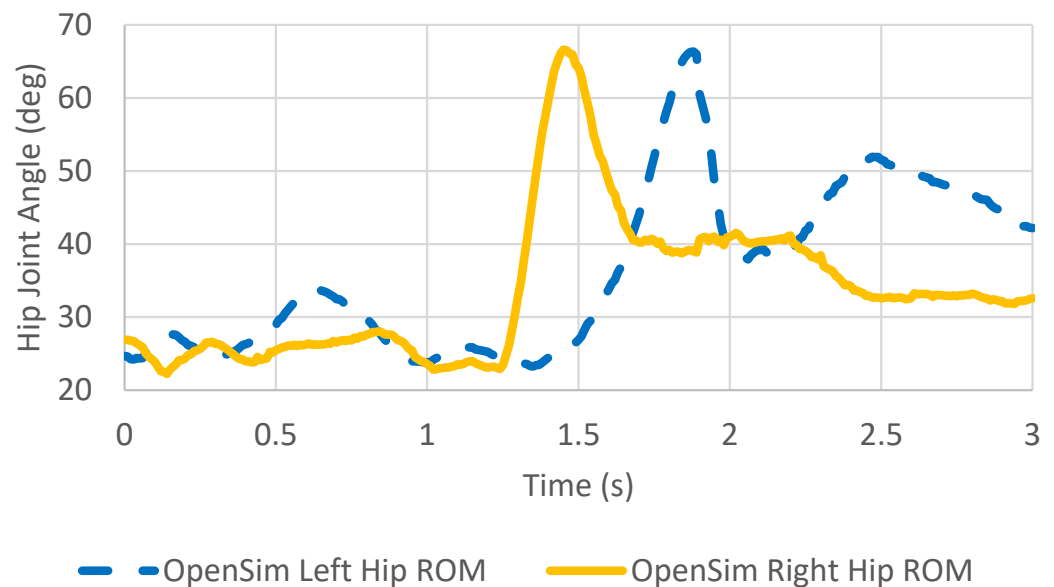


**Figure 3.** Hip joint ROM for left and right hips over a 3 s period.

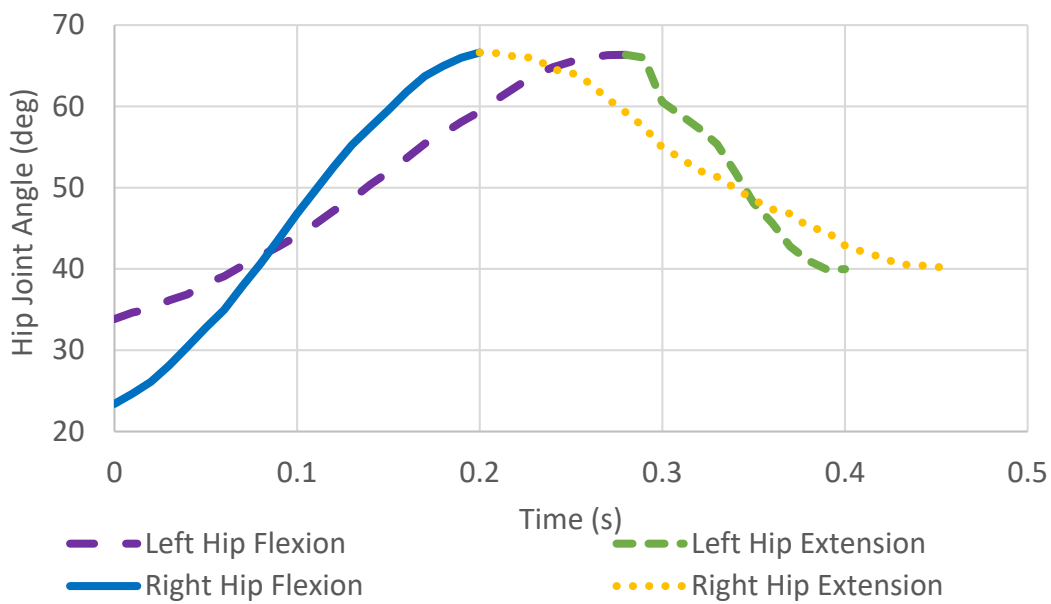


**Figure 4.** Hip joint angle data during discrete isolated kicks for right and left hips.

3.2. Hip Joint Moment

The correlating hip joint moment results of the discrete kicks for the right and left hip joints are shown in Figure 5 and are consistent with the observed hip ranges of motion. Figure 5 shows that the maximum torque is required at the beginning of the kick cycle when the hip joint torque must overcome the gravitational force to reach maximum flexion. Once the gravitational force is overcome, the moment decreases to slow down the motion as it reaches maximum flexion. Similarly, the moment increases as the motion reverses as it goes into extension where the maximum torque is needed at the end of the kick cycle to slow down the hip joint.

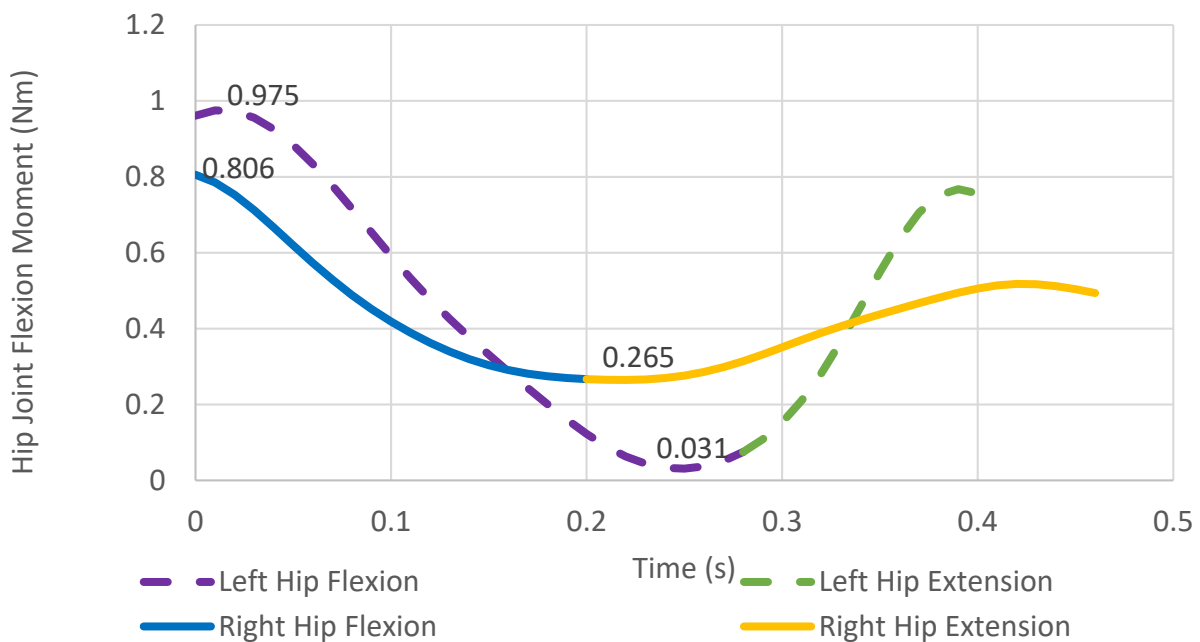


**Figure 5.** Hip joint moment during discrete isolated kicks for right and left hips.

4. Discussion

The purpose of this study was to create a preliminary musculoskeletal computational model representative of an infant to study the biomechanics of the lower extremity. By



using experimental motion-capture data along with external forces, a novel musculoskeletal model was created using inverse kinematics and dynamics. Our preliminary results suggest that the musculoskeletal model is able to portray the biomechanics of infants when estimating hip joint ROM and moments to investigate healthy infant movement.

Our results for the hip flexion angle and hip moment were normalized by the time scale to better compare the kicks with varying kick duration to the kicks reported in the literature [33]. Figure 6 shows a trend agreement between the reported values and our results. However, reported flexion values were higher when compared to our model. There was a maximum hip joint angle difference of  $30.5^\circ$  (right hip) and  $30.8^\circ$  (left hip) when compared to the literature. This maximum difference was observed at the corresponding time of maximum hip flexion angle. This difference is attributed to dissimilarities in data collection methodologies and subject heterogeneity. In the methods used by Schneider et al. [33], the infant subject's chest and abdomen were immobilized while the lower extremity could move freely and naturally. On the other hand, our study permitted no movement restrictions, allowing the upper extremity as well as the lower extremity to move freely and naturally in coordination with the upper body. With these different approaches, we see that the kick cycle ends at a greater hip joint angle for both hips compared to the starting hip joint angle at the beginning of the kick cycle. This may be caused by the additional muscle control needed when motion is reversed from flexion to extension to stabilize the hip joint.

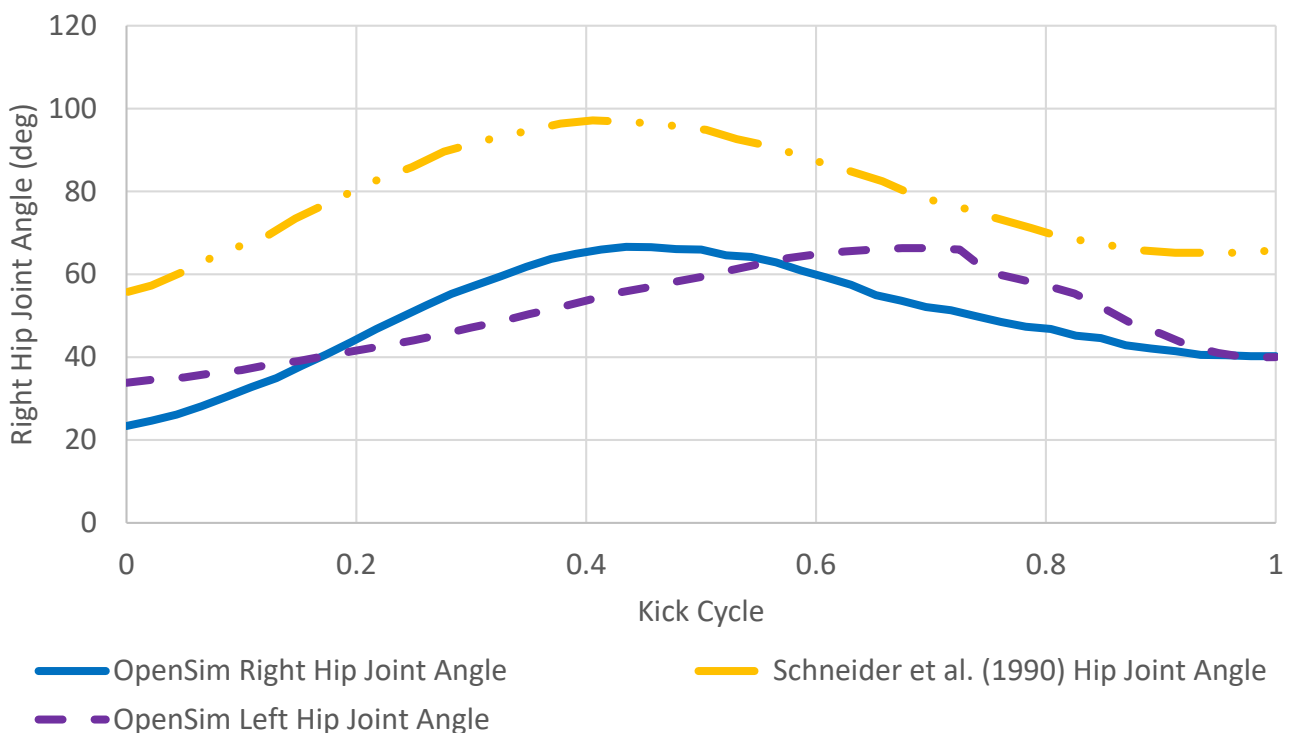


**Figure 6.** Time normalized hip joint ROM comparison between infant model and Schneider et al.'s [33].

Hip joint moment data obtained through the musculoskeletal model were also normalized and compared to values reported in the literature [33]. In both results, a decrease in moment was observed during hip flexion, and an increase in moment was observed during the extension of the hip, as shown in Figure 7.

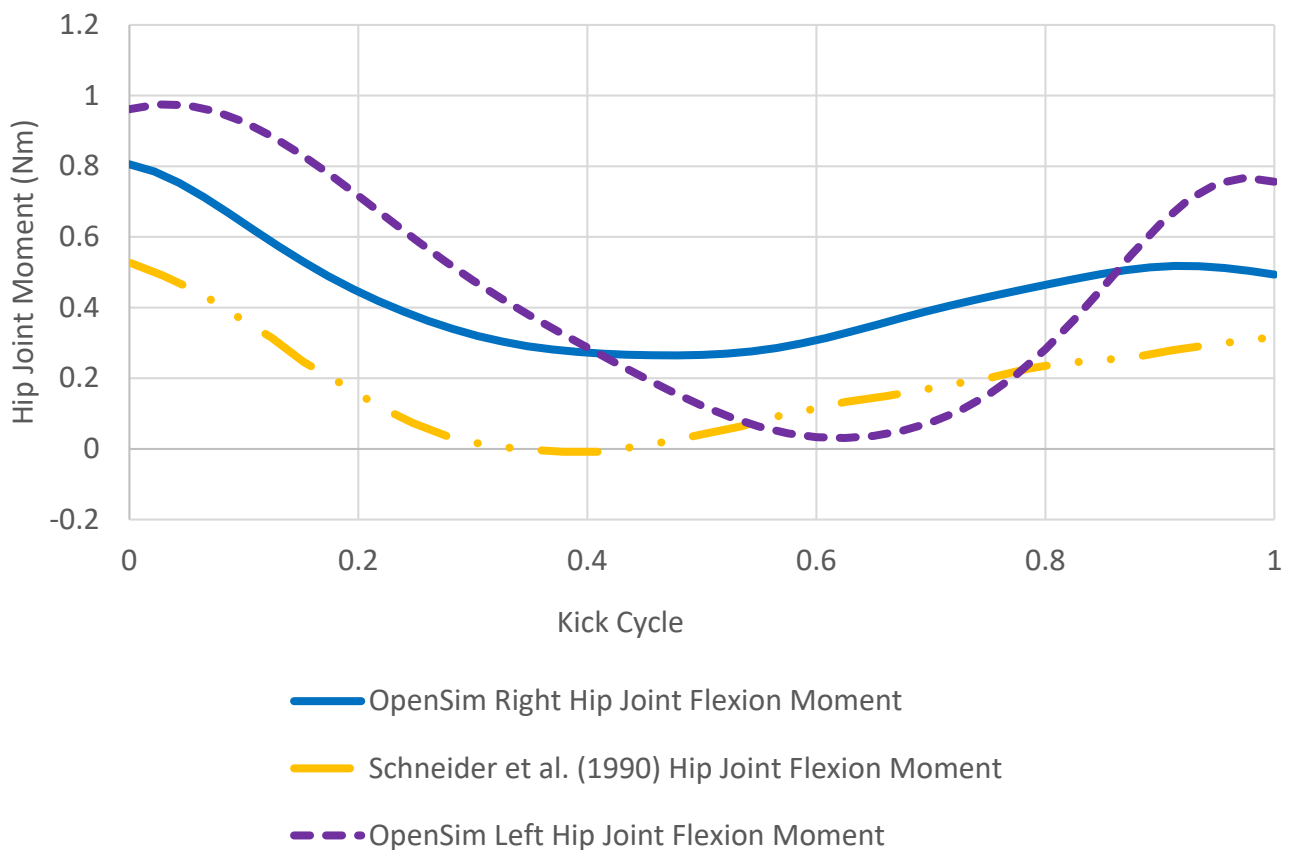


**Figure 7.** Normalized hip joint moment comparison between infant model and Schneider et al.'s [33].

Figure 7 shows hip joint moment for both the right and left hip decreases as the hip joint undergoes flexion and then increases as the hip returns to the extended position. The flexion phase of the kick corresponds to concentric hip flexor contraction, while the extension phase corresponds to eccentric hip flexor contraction. This trend coincides with the results found in Schneider et al.'s study in their joint moment calculations [33]. Similar to the comparison made on the hip joint angle, a trend agreement was observed when comparing moment values from the infant model to reported values from the literature [33]. There was a hip joint moment difference of 0.275 Nm (right hip) and 0.083 Nm (left hip) when compared to the literature. This maximum difference (right: 0.283 Nm; left: 0.039 Nm) was observed at the corresponding time of maximum hip flexion angle. The difference in moments can be attributed to several factors, such as not restraining the upper extremity, the difference in kick intensity, and that the present model was developed from subject-specific data.

Due to the limitation of accessible data, and the fact that infant subjects are unable to follow verbal instructions, recreating specific kicking motions is impossible. The similarity in how the joint moment behaves with respect to hip joint flexion and extension is observed in both the results of this study and results found in the literature.

Another limitation of this study is that the regression equations were based on child and adult populations ranging between the ages of 5-years-old and 40-years-old [31]. There are currently no regression equations present in the literature for estimating the location of hip joint centers in infants. Regression equations are developed using either cadaveric data or medical imaging studies [34]. To the knowledge of the authors, such data for infant populations under the age of one year old are not available. The risks of radiation exposure from taking CT scans of young, healthy infants to obtain more representative regression equations are not justifiable. Other approaches that do not include ionizing radiation, including MRI scans or ultrasound, were outside of the scope of this study. Nonetheless, amongst the regression methods, Hara et al. [31] found an improved accuracy of their

regression equations when compared to previously published equations [35–37] when using the leg length as the predictor. Furthermore, the Hara method had the largest sample size of all regression methods for estimating hip joint centers. Exploring the best methods of defining the HJC for an infant population should be a focus of future research.

The paucity of infant biomechanical data in the literature is a major limitation in infant musculoskeletal modeling. Additionally, infants' inability to follow instructions in an experimental laboratory makes infant biomechanics research a unique challenge. Our model, while not yet generalizable to the infant population, represents a crucial advance in developing subject-specific infant lower-extremity MCM from experimental data.

This study represents a novel musculoskeletal model that can enable innovative research on the understudied infant population and eventually extend to pathologies such as DDH. Eventually, researchers with limited or no access to infant participants will be able to use the infant MCM model to study biomechanical loads that occur at the hip joint during dynamic movements and use the results to identify and evaluate the mechanisms that contribute to infant hip development. Future work should include how joint moments might change with age during the first year of life before infants start walking. During this period, the anatomy and neuromuscular system of infants undergo rapid changes, making the development of valid subject-specific MCM of infants a crucial step to gain a more granular and holistic understanding of infant growth and development.

## 5. Conclusions

A preliminary musculoskeletal computational model representative of an infant to study the biomechanics of the lower extremity was created. This novel musculoskeletal model was created using experimental MOCAP and GRF data, as well as OpenSim's inverse kinematics and inverse dynamics post-processing tools. The infant MCM can enable innovative research on the understudied infant population by providing more insight into biomechanical loadings at the hip joint during a spontaneous kick and can eventually be extended to evaluating the mechanisms contributing to pathologies such as DDH.

**Author Contributions:** Conceptualization, V.H. and E.M.; methodology, E.M., S.S., V.H., Y.L. and C.W.; software, Y.L., T.C. and C.W.; validation, Y.L. and T.C.; formal analysis, Y.L., T.C., V.H., E.M., S.S. and C.W.; investigation, Y.L. and T.C.; resources, E.M., S.S. and V.H.; data curation, Y.L. and T.C.; writing—original draft preparation, Y.L., T.C., V.H., E.M., S.S. and C.W.; writing—review and editing, T.C., V.H., E.M. and S.S.; visualization, Y.L. and T.C.; supervision, V.H. and E.M.; project administration, V.H.; funding acquisition, E.M. and V.H. All authors have equally contributed to this paper. All authors have read and agreed to the published version of the manuscript.

**Funding:** This study was supported in part by Boba, Inc., the International Hip Dysplasia Institute, NIH P20GM125503, and internal funds.

**Conflicts of Interest:** The authors declare no conflict of interest.

## References

1. Matsuo, T.; Fleisig, G.S.; Zheng, N.; Andrews, J.R. Influence of shoulder abduction and lateral trunk tilt on peak elbow varus torque for college baseball pitchers during simulated pitching. *J. Appl. Biomech.* **2006**, *22*, 93–102. [PubMed]
2. Walck, C.; Huayamave, V.; Osbahr, D.; Furman, T.; Farnese, T. A Patient-Specific Lower Extremity Biomechanical Analysis of a Knee Orthotic during a Deep Squat Movement. *Med. Eng. Phys.* **2020**, *80*, 1–7.
3. Dao, T.; Marin, F.; Pouletaut, P.; Charleux, F.; Aufaure, P.; Ho Ba Tho, M. Estimation of accuracy of patient-specific musculoskeletal modelling: Case study on a post polio residual paralysis subject. *Comput. Methods Biomech. Biomed. Eng.* **2012**, *15*, 745–751.
4. Gaffney, B.M.; Hillen, T.J.; Nepple, J.J.; Clohisy, J.C.; Harris, M.D. Statistical shape modeling of femur shape variability in female patients with hip dysplasia. *J. Orthop. Res.* **2019**, *37*, 665–673.
5. Marra, M.A.; Vanheule, V.; Fluit, R.; Koopman, B.H.; Rasmussen, J.; Verdonshot, N.; Andersen, M.S. A subject-specific musculoskeletal modeling framework to predict in vivo mechanics of total knee arthroplasty. *J. Biomech. Eng.* **2015**, *137*, 020904.
6. Rahman, M.; Cil, A.; Bogener, J.W.; Stylianou, A.P. Lateral collateral ligament deficiency of the elbow joint: A modeling approach. *J. Orthop. Res.* **2016**, *34*, 1645–1655.

7. Song, K.; Anderson, A.E.; Weiss, J.A.; Harris, M.D. Musculoskeletal models with generic and subject-specific geometry estimate different joint biomechanics in dysplastic hips. *Comput. Methods Biomech. Biomed. Eng.* **2019**, *22*, 259–270.
8. Thomas-Aitken, H.D.; Goetz, J.E.; Dibbern, K.N.; Westermann, R.W.; Willey, M.C.; Brown, T.S. Patient age and hip morphology alter joint mechanics in computational models of patients with hip dysplasia. *Clin. Orthop. Relat. Res.* **2019**, *477*, 1235–1245.
9. Alizadeh, M.; Knapik, G.G.; Mageswaran, P.; Mendel, E.; Bourekas, E.; Marras, W.S. Biomechanical musculoskeletal models of the cervical spine: A systematic literature review. *Clin. Biomech.* **2020**, *71*, 115–124.
10. Ghezelbash, F.; Shirazi-Adl, A.; Arjmand, N.; El-Ouaaid, Z.; Plamondon, A. Subject-specific biomechanics of trunk: Musculoskeletal scaling, internal loads and intradiscal pressure estimation. *Biomech. Model. Mechanobiol.* **2016**, *15*, 1699–1712.
11. Rasmussen, J.; Tørholm, S.; de Zee, M. Computational analysis of the influence of seat pan inclination and friction on muscle activity and spinal joint forces. *Int. J. Ind. Ergon.* **2009**, *39*, 52–57.
12. Mundt, M.; Koeppe, A.; David, S.; Bamer, F.; Potthast, W.; Markert, B. Prediction of ground reaction force and joint moments based on optical motion capture data during gait. *Med. Eng. Phys.* **2020**, *86*, 29–34.
13. Kong, P.W.; Pan, J.W.; Chu, D.P.K.; Cheung, P.M.; Lau, P.W.C. Acquiring expertise in precision sport: What can we learn from an elite snooker player? *Phys. Act. Health* **2021**, *5*, 98–106.
14. Sylvester, A.D.; Lautzenheiser, S.G.; Kramer, P.A. A review of musculoskeletal modelling of human locomotion. *Interface Focus* **2021**, *11*, 20200060.
15. Verbruggen, S.W.; Loo, J.H.; Hayat, T.T.; Hajnal, J.V.; Rutherford, M.A.; Phillips, A.T.; Nowlan, N.C. Modeling the biomechanics of fetal movements. *Biomech. Model. Mechanobiol.* **2016**, *15*, 995–1004.
16. Nowlan, N.C. Biomechanics of foetal movement. *Eur. Cell Mater.* **2015**, *29*, 21.
17. Chen, H.; Song, Y.; Xuan, R.; Hu, Q.; Baker, J.S.; Gu, Y. Kinematic Comparison on Lower Limb Kicking Action of Fetuses in Different Gestational Weeks: A Pilot Study. *Healthcare* **2021**, *9*, 1057.
18. Zwawi, M.A.; Moslehy, F.A.; Rose, C.; Huayamave, V.; Kassab, A.J.; Divo, E.; Jones, B.J.; Price, C.T. Developmental dysplasia of the hip: A computational biomechanical model of the path of least energy for closed reduction. *J. Orthop. Res.* **2016**, *35*, 1799–1805. [[CrossRef](#)]
19. Huayamave, V.; Rose, C.; Serra, S.; Jones, B.; Divo, E.; Moslehy, F.; Kassab, A.J.; Price, C.T. A patient-specific model of the biomechanics of hip reduction for neonatal Developmental Dysplasia of the Hip: Investigation of strategies for low to severe grades of Developmental Dysplasia of the Hip. *J. Biomech.* **2015**, *48*, 2026–2033.
20. Huayamave, V.; Lozinski, B.; Rose, C.; Ali, H.; Kassab, A.; Divo, E.; Moslehy, F.; Price, C. Biomechanical evaluation of femoral anteversion in developmental dysplasia of the hip and potential implications for closed reduction. *Clin. Biomech.* **2020**, *72*, 179–185.
21. Bialik, V.; Bialik, G.M.; Blazer, S.; Sujov, P.; Wiener, F.; Berant, M. Developmental Dysplasia of the Hip: A New Approach to Incidence. *Pediatrics* **1999**, *103*, 93–99.
22. Dezateux, C.; Rosendahl, K. Developmental dysplasia of the hip. *Lancet* **2007**, *369*, 1541–1552.
23. Ortiz-Neira, C.L.; Paolucci, E.O.; Donnon, T. A meta-analysis of common risk factors associated with the diagnosis of developmental dysplasia of the hip in newborns. *Eur. J. Radiol.* **2012**, *81*, e344–e351.
24. Bahl, J.S.; Zhang, J.; Killen, B.A.; Taylor, M.; Solomon, L.B.; Arnold, J.B.; Lloyd, D.G.; Besier, T.F.; Thewlis, D. Statistical shape modelling versus linear scaling: Effects on predictions of hip joint centre location and muscle moment arms in people with hip osteoarthritis. *J. Biomech.* **2019**, *85*, 164–172. [[PubMed](#)]
25. Kainz, H.; Carty, C.P.; Maine, S.; Walsh, H.P.J.; Lloyd, D.G.; Modenese, L. Effects of hip joint centre mislocation on gait kinematics of children with cerebral palsy calculated using patient-specific direct and inverse kinematic models. *Gait Posture* **2017**, *57*, 154–160. [[PubMed](#)]
26. Kainz, H.; Hoang, H.X.; Stockton, C.; Boyd, R.R.; Lloyd, D.G.; Carty, C.P. Accuracy and reliability of marker-based approaches to scale the pelvis, thigh, and shank segments in musculoskeletal models. *J. Appl. Biomech.* **2017**, *33*, 354–360. [[PubMed](#)]
27. Siddicky, S.F.; Bumpass, D.B.; Krishnan, A.; Tackett, S.A.; McCarthy, R.E.; Mannen, E.M. Positioning and baby devices impact infant spinal muscle activity. *J. Biomech.* **2020**, 109741.
28. Siddicky, S.F.; Wang, J.; Rabenhorst, B.; Buchele, L.; Mannen, E.M. Exploring infant hip position and muscle activity in common baby gear and orthopedic devices. *J. Orthop. Res.* **2020**, *39*, 941–949.
29. Delp, S.L.; Anderson, F.C.; Arnold, A.S.; Loan, P.; Habib, A.; John, C.T.; Guendelman, E.; Thelen, D.G. OpenSim: Open-source software to create and analyze dynamic simulations of movement. *Biomed. Eng. IEEE Trans.* **2007**, *54*, 1940–1950.
30. Seth, A.; Hicks, J.L.; Uchida, T.K.; Habib, A.; Dembia, C.L.; Dunne, J.J.; Ong, C.F.; DeMers, M.S.; Rajagopal, A.; Millard, M. OpenSim: Simulating musculoskeletal dynamics and neuromuscular control to study human and animal movement. *PLoS Comput. Biol.* **2018**, *14*, e1006223.
31. Hara, R.; McGinley, J.; Briggs, C.; Baker, R.; Sangeux, M. Predicting the location of the hip joint centres, impact of age group and sex. *Sci. Rep.* **2016**, *6*, 37707.
32. Kliegman, R.M.; Behrman, R.E.; Jenson, H.B.; Stanton, B.M. *Nelson Textbook of Pediatrics e-Book*; Elsevier Health Sciences: Amsterdam, The Netherlands, 2007.
33. Schneider, K.; Zernicke, R.F.; Ulrich, B.D.; Jensen, J.L.; Thelen, E. Understanding movement control in infants through the analysis of limb intersegmental dynamics. *J. Mot. Behav.* **1990**, *22*, 493–520.

34. Kainz, H.; Hajek, M.; Modenese, L.; Saxby, D.J.; Lloyd, D.G.; Carty, C.P. Reliability of functional and predictive methods to estimate the hip joint centre in human motion analysis in healthy adults. *Gait Posture* **2017**, *53*, 179–184.
35. Bell, A.L.; Brand, R.A.; Pedersen, D.R. Prediction of hip joint centre location from external landmarks. *Hum. Mov. Sci.* **1989**, *8*, 3–16.
36. Davis Iii, R.B.; Ounpuu, S.; Tyburski, D.; Gage, J.R. A gait analysis data collection and reduction technique. *Hum. Mov. Sci.* **1991**, *10*, 575–587.
37. Harrington, M.E.; Zavatsky, A.B.; Lawson, S.E.M.; Yuan, Z.; Theologis, T.N. Prediction of the hip joint centre in adults, children, and patients with cerebral palsy based on magnetic resonance imaging. *J. Biomech.* **2007**, *40*, 595–602.